SEISMOELECTRIC AND SEISMOMAGNETIC MEASUREMENTS IN FRACTURED BOREHOLE MODELS

Zhenya Zhu and M.Nafi Toksöz

Earth Resources Laboratory
Department of Earth, Atmospheric, and Planetary Sciences
Massachusetts Institute of Technology
Cambridge, MA 02139

ABSTRACT

Seismoelectric and seismomagnetic fields generated by acoustic waves in fluid-saturated fractured borehole models are experimentally investigated with an electrode and a Hall-effect sensor. In a borehole with a horizontal fracture, the Stoneley and flexural waves induce seismoelectric and seismomagnetic fields on the borehole wall and an electromagnetic wave propagating with light speed at the horizontal fracture. In a borehole with a vertical fracture, the acoustic field generated by a monopole or dipole source is similar to that in a borehole without a vertical fracture. However, the acoustic wave propagating along the vertical fracture induces seismoelectric and seismomagnetic fields, whose apparent velocities are equal to that of a Stoneley wave. Experimental results show that two different kinds of electric and magnetic fields are generated by acoustic waves in borehole models with horizontal and/or vertical fractures. One is an electromagnetic wave propagating with light speed. The second is a stationary or localized seismoelectric and seismomagnetic field. Seismoelectric and seismomagnetic measurements might be a new logging technique for exploring fractures in a borehole.

INTRODUCTION

At a solid-fluid interface of a porous medium or a fluid-saturated fracture, adsorption of an electric charge to the solid surface creates an excess of mobile ions of opposite charge to that of the fluid (Bockris and Reddy, 1970). Thus, a double layer is formed on the solid surface. When a seismic wave propagates in a two-phase medium of solid and fluid, the particle vibration generates a movement of ions in the fluid that induces an electric, magnetic field, or electromagnetic field (Haartsen, 1995). This phenomenon—that a

seismic wave induces an electric field—is referred to as seismokinetic or seismoelectric conversion.

Early theoretical studies (Fitterman, 1978, 1979) investigated the electrokinetic and magnetic field or anomalies due to fluid motion along a fault. Recent theoretical studies (Fenoglio *et al.*, 1995; Haartsen, 1995; Pride and Haartsen, 1996) confirm the mechanism of the conversion. Inside a homogeneous, porous medium, the seismic wave induces localized seismoelectric and seismomagnetic fields which exist only in the area disturbed by the seismic wave. At an interface of material with different properties, such as porosity, permeability or lithology, the seismic wave induces a radiating seismoelectric wave or electromagnetic wave, which propagates with light speed and can be received anywhere.

Many laboratory experiments have studied the seismoelectric field and its properties generated by stable fluid flow or low-frequency vibration (Morgan *et al.*, 1989). The experiments in borehole models (Zhu and Toksöz, 1997, 1998) show that two different kinds of electric fields are induced by a Stoneley wave in a fluid-saturated, fractured borehole. The previous experiments have not directly measured the magnetic field generated by an acoustic wave and predicted by theoretical studies (Haartsen, 1995; Fenoglio *et al.*, 1995).

Many field experiments have measured the seismoelectric signals on the ground (Thompson and Gist, 1993; Butler *et al.*, 1996; Mikhailov *et al.*, 1997). In these experiments, the seismic source is on the ground and the electrode is in the borehole during the borehole measurements. Because the seismoelectric conversion efficiency is very low, these measurements cannot reach a deep formation. Mikhailov (1998) has conducted electroseismic logging in a borehole. Both source and four receivers (electrodes) were placed in the borehole.

In this paper, we conduct a series of experiments to study the seismoelectric, seismomagnetic and electromagnetic fields induced by a monopole or dipole source and the effects of horizontal and vertical fractures on the fields.

MEASUREMENTS IN A BOREHOLE WITH A HORIZONTAL FRACTURE

A borehole model with a horizontal fracture is shown in Figure 1. To simulate a horizontal fracture intersecting a borehole, we make a borehole model with two separate blocks, one Lucite and one slate. The aperture of the fracture between the two blocks is about 0.05 mm. The diameter of the borehole is about 10 mm. The whole model is placed into a water tank and saturated with water of 65 μS in conductivity.

A mono/dipole transducer, 9.0 mm in diameter, is placed at the lower section of the slate and excited by an electric square pulse of 10 μs in width and 750 V in amplitude. By moving along the borehole, three kinds of sensors—acoustic transducer, electrode and a Hall-effect sensor—measure acoustic, electric and magnetic fields. After going though a pre-amplifier with 60-db gain and a filter of 1 kHz-200 kHz bandwidth, the

received signals are displayed and recorded on a digital oscilloscope (Zhu and Toksöz, 1996). Both the acoustic source and receiver are mono/dipole transducers which can work as either monopole or dipole transducers.

Acoustic Field

Figure 2 shows the acoustic waves generated and received by monopole (Figure 2a) or dipole (Figure 2b) transducers. There is a time delay of 32 μs for each trace in the records. The monopole source generates a very strong Stoneley wave (Figure 2a). After propagating through the horizontal fracture, which is located between traces 5 and 6, the Stoneley wave generates a P-wave and Stoneley wave in the Lucite section. This result confirms that there is a water-saturated fracture between the slate and Lucite. The velocities of Stoneley waves in slate and Lucite are 1400 m/s and 1050 m/s, respectively.

In Figure 2b, we see that the first arrival in the slate section is a fast flexural wave, whose velocity is close to that of the fast shear wave. The dipole source also generates a very strong flexural guided wave, whose velocity (1540 m/s) is a little higher than water's velocity (1480 m/s). This flexural guided wave is different from a Stoneley wave not only in velocity but also in vibration mode. After propagating across the horizontal fracture (trace 5), the flexural guided wave generates a Stoneley wave (traces 6–16) in the Lucite section. This also implies that there is a water-saturated fracture located between traces 5 and 6 (Figure 2).

Seismoelectric Field

Figure 3 shows the seismoelectric signals generated by monopole (Figure 3a) and dipole (Figure 3b) sources and received by an electrode 3 mm in length and 9 mm in diameter in the borehole model with a horizontal fracture. There is a time delay of 64 μs for each trace in Figure 3 and all of the following records to avoid the electronical influence of the source pulse. The amplitude is normalized for each plot. From traces 1–5 in Figure 3a, we see that the Stoneley wave induces an electric signal, whose apparent velocity is the same as the Stoneley wave. At the fracture, the Stoneley wave induces an electric wave. Because the arrival times are exactly the same in traces 6–16, this wave should be an electromagnetic wave and the recorded signals are its electric component. Most of the electric signals generated by the Stoneley wave at the fracture are caused by the propagating electromagnetic wave. No signal propagating with Stoneley wave velocity is received in the Lucite section.

Figure 3b shows the seismoelectric field generated by the flexural guided wave, and the field is similar to that generated by a monopole source. At the horizontal fracture, a strong electric signal with the speed of light is induced, but no signal with Stoneley wave velocity is recorded in the Lucite section. Because the flexural wave propagating with shear wave velocity does not generate any measurable electric signal, we do not record or study it in this paper.

The amplitude of the electromagnetic wave induced at a horizontal fracture depends on the aperture of the fracture (Zhu and Toksöz, 1998). The smaller the aperture, the larger the amplitude of the electromagnetic wave. In this experiment, the aperture of 0.05 mm is very small, so the main signal is the electromagnetic wave. We do not observe the electric signal induced by the Stoneley wave in the Lucite section due to its small amplitude.

Comparing the waveforms in Figure 3a with Figure 3b, we see that the waveform and the center frequency are different from each other and the frequency difference is larger than that between the acoustic waves in Figures 2a and 2b. Therefore, the seismoelectric conversion efficiencies of the Stoneley wave and the flexural guided wave are different, and there may be a relaxation for the seismoelectric conversion of the Stoneley wave. Our experiment cannot determine which component of the acoustic vibration generates the electric signal.

Magnetic Field

A Hall-effect device, as a receiver, measures the magnetic field generated by a monopole source in the model. The Hall effect, discovered by E. F. Hall in 1879, is the basis for the Hall-effect device. When this physical effect is combined with modern integrated circuit (IC) technology, the device becomes more useful for detecting magnetic fields. A functional diagram of a Hall-effect device of Model A3515LUA made by Allegro MicroSystem, Inc. is shown in Figure 4a. The size of the device is $4.1 \times 3.1 \times 1.5cm^3$. A Hall-effect sensor is located in the center of the device. Its output voltage is proportional to the magnetic flux through the sensor and related to the direction of the flux. A typical output of the device A3515LUA is shown in Figure 4b.

In our experiment the supply voltage V_{cc} is 5.0 V. The DC output is 2.5 V when there is no magnetic field. Only the alternating signal can go through the preamplifier and the filter. We fix the Hall-effect device on the end of a stick 6 mm in diameter to keep its plane of $4.1mm \times 3.1mm$ parallel (Figure 5a) or perpendicular (Figure 5b) to the borehole axis. When the device moves along the borehole, it may receive the magnetic component which is perpendicular or parallel to the borehole axis. The Hall-effect device and its connecting wires are electrically isolated from the borehole fluid during the measurement. The Hall-effect sensor is not sensitive to the magnetic component of an electromagnetic wave.

Figure 6 shows the magnetic signals generated by a monopole source and received by a vertical (Figure 6a) or horizontal (Figure 6b) Hall-effect device. In the slate section, we recorded magnetic signals, which are about 10 μV in maximum amplitude and about 120 kHz in center frequency. The propagating velocity is equal to the Stoneley wave velocity in slate. In traces 6–16 in Figure 6, we do not record any measurable signals which propagate at light speed or Stoneley wave velocity in the Lucite section.

The results confirm that the signals in Figure 3a are two kinds of electric signals with different properties. The signal generated at the horizontal fracture, propagating at light speed and not received by the Hall-effect sensor, should be an electromagnetic

wave. In the slate section, there is a stationary electric and magnetic field. We know that the magnetic field is a vector and the output of the Hall-effect device is proportional to the magnetic flux perpendicular to the sensor surface. When we measure the magnetic field in a borehole, three components of the field can be recorded and can obtain more information about seismokinetic conversion. Because the device is electrically isolated from the borehole fluid, it is simple to install it into a downhole tool.

MEASUREMENTS IN A BOREHOLE WITH A VERTICAL FRACTURE

To investigate and compare the effects of horizontal and vertical fractures on the seismoelectric field and seismomagnetic field in a fluid-saturated borehole, we make a borehole model (Figure 7) with a vertical fracture on the basis of the previous borehole model, with a horizontal fracture. There is a horizontal fracture between the two blocks as in Figure 1 and a vertical fracture with 0.25 mm in aperture in the Lucite section. All of the measurements in this paragraph are the same as for the horizontal fracture.

Aoustic Field

Figure 8 shows the acoustic waveforms generated by a monopole source (Figure 8a) and the waveforms generated by a dipole source (Figure 8b) in the borehole with a vertical fracture. Because we are more interested in the seismoelectric and seismomagnetic field generated by a Stoneley wave and a flexural guided wave, we do not record parts of the shear wave or fast flexural wave at a 64μs time delay for each trace. From Figure 8a, we see that the Stoneley wave propagates across the horizontal fracture and generates P-wave and Stoneley waves in the Lucite section. Comparing them with those in Figure 2, we could not see a big difference or the effect of the vertical fracture on the acoustic field in the Lucite section.

Seismoelectric Field

Figure 9 shows the seismoelectric fields generated by a monopole source (Figure 9a) and a dipole source (Figures 9b and 9c), and received by an electrode in the borehole with a vertical fracture. From Figure 9a, we see three kinds of seismoelectric fields. There is a seismoelectric signal propagating with the velocity of a Stoneley wave in the slate section (traces 1–5). There is an electromagnetic wave propagating with light speed in the Lucite section (traces 6–16). Both of them are the same as those in the horizontal fracture model (Figure 3a). However, we also observe the third electric field propagating with the Stoneley wave velocity in the Lucite section (traces 10–16). This third field is not found in the model with horizontal fracture (compare Figures 9a and 3a), although the Stoneley waves propagating along the borehole wall in the Lucite sections are recorded in both models (Figures 2a and 8a). We conclude that the third field recorded in the vertical fracture borehole is generated by the Stoneley wave

propagating along the vertical fracture instead of the Stoneley wave along the borehole wall.

From the shape and frequency of the recorded electric signals in Figure 9a, the frequency of the first arrival is close to the center frequency (120 kHz) of the acoustic wave, but that of the following waveforms decrease. This phenomenon indicates a possible relaxation responsibility in the seismoelectric conversion.

The seismoelectric signals generated by a dipole source are recorded when the plane of the vertical fracture is parallel (Figure 9b) or perpendicular (Figure 9c) to the main direction of the dipole source. The principal characteristics of the three seismoelectric fields in Figures 9a and 9c are similar to those generated by a monopole source in Figure 9a. The frequency is close to the center frequency (120 kHz) of the flexural wave.

The experimental results show that the Stoneley wave generates two kinds of seismoelectric signals—an electromagnetic wave and a stationary or localized seismoelectric field, at horizontal and vertical fractures, respectively.

Magnetic Field

Figure 10 shows the seismomagnetic signals generated by a monopole source and received by a Hall-effect device positioned vertically (Figure 10a) or horizontally (Figure 10b) in the borehole with a vertical fracture. Two magnetic components of the seismomagnetic field are recorded in the slate section (traces 1–5 in Figures 10a and 10b). The center frequency of the magnetic field is close to that of the Stonely wave. In the Lucite section, we do not record any magnetic wave propagating with light speed, the same as that which we observe in Figures 6a and 6b. However, we record magnetic signals propagating with P-wave velocity (traces 6–16 in Figure 10a) and with Stoneley wave velocity (traces 6–16 in Figure 10b) in the Lucite section. Particularly, the amplitude of the magnetic signal is very clear in Figure 10b. In both models (Figures 1 and 7), we record strong Stoneley waves propagating along the borehole walls (Figures 2a and 8a), but we do not record a clear magnetic signal in the Lucite section of the horizontal fracture model (Figures 6a and 6b). Therefore, this magnetic signal (Figure 10) is formed at the intersection of the horizontal and vertical fractures and generated by the Stoneley wave propagating along the vertical fracture. It is a stationary or localized seismomagnetic field.

The different particle motions of the P-wave and Stoneley wave induce the different kinds and amplitudes of the two magnetic components in Figures 10a and 10b. Three-component measurements of the magnetic field will provide more information to investigate fractures at different angles or more complex fractures.

CONCLUSIONS

We investigated the seismokinetic conversion induced by a monopole or dipole source in borehole models with a horizontal or vertical fracture experimentally. We measured the acoustic, electric and magnetic fields with a mono/dipole, an electrode and a Hall-effect device in the models, respectively. The acoustic wave responded to a horizontal fracture so strongly that the Stoneley wave or flexural guided wave generated a P-wave and Stoneley wave at the fracture. However, the acoustic wave did not respond to a vertical fracture because most of acoustic energy propagates along the borehole wall where there is no vertical fracture.

Because the horizontal fracture forms a discontinuous interface on the propagation direction of the acoustic wave, the flow of the mobile charges in the fracture fluid generated by the acoustic wave induces an electromagnetic wave propagating with light speed. Because there is no interface along the propagation direction of the acoustic wave in the borehole with a vertical fracture, the acoustic wave propagating along the vertical fracture induces a stationary or localized seismoelectric field in the section with a vertical fracture.

The Hall-effect device used in our experiments is a magnetic sensor whose output is proportional to the magnetic flux density and the direction of the magnetic field. This device does not respond to the magnetic component of any electromagnetic wave. Although a Stoneley wave induces a strong electromagnetic wave at a horizontal fracture, the Hall-effect sensor does not receive any magnetic component of the electromagnetic wave. In the borehole with a vertical fracture, a magnetic field is induced by the Stonely wave propagating along the fracture instead of the borehole wall. It is possible that the multicomponent magnetic measurement can provide more information about an inclined or complex fracture intersecting a borehole.

Our experiments show that the seismoelectric and seismomagnetic measurements in a fluid-saturated borehole can provide more information about fracture distribution than traditional acoustic logging. The seismoelectric and seismomagnetic measurement could be a new logging method.

ACKNOWLEDGMENTS

We would like to thank Drs. Art Thompson, Dan Burns, Matthijs Haartsen, and Prof. Steven Pride for their valuable suggestions and useful discussions.

This work was supported by the Borehole Acoustics and Logging/Reservoir Delineation Consortia at the Massachusetts Institute of Technology.

REFERENCES

Bockris. J., and Reddy, A.K.N., 1970, *Modern Electrochemistry,* Plenum Press.

Butler, K., Russell, R., Kepic, A., and Maxwell, M., 1996, Measurement of the seismoelectric response from a shallow boundary, *Geophysics, 61*, 1769–1778.

Fenoglio, M.A., Johnston, M.J.S., and Byerlee, J.D., 1995, Magnetic and electric fields associated with changes in high pore pressure in fault zones: Application to the Loma Prieta ULF emissions, *J. Geophys. Res., 100*, 12951–12958.

Fitterman, D.V., 1978, Electrokinetic and magnetic anomalies associated with dilatant regions in a layered earth, *J. Geophys. Res., 83*, 5923–5928.

Fitterman, D.V., 1979, Theory of electrokinetic-magnetic anomalies in a faulted half-space, *J. Geophys. Res., 84*, 6031–6040.

Haartsen, M.W., 1995, Coupled electromagnetic and acoustic wavefield modeling in poro-elastic media and its application in geophysical exploration, Ph.D. Thesis, MIT.

Mikhailov, O.V., Haartsen, M.W., and Toksöz, M.N., 1997, Electroseismic investigation of the shallow subsurface: Field measurements and numerical modeling, *Geophysics, 62.*, 97–105.

Mikhailov, O.V., 1998, Borehole electroseismic phenomena: Field measurements and theory, Ph.D. Thesis, MIT.

Pride, S.R., and Haartsen, M.W., 1996, Electroseismic wave properties, *J. Acoust. Soc. Am., 100*, 1301–1315.

Morgan, F.D., Williams, E.R., and Madden, T.R., 1989, Streaming potential properties of Westerly Granite with applications, *J. Geophys. Res., 94*, 12449–12461.

Thompson, A.H., and Gist, G.A., 1993, Geophysical applications of electrokinetic conversion, *The Leading Edge, 12*, 1169–1173.

Zhu, Z., and Toksöz, M.N., 1996, Experimental studies of seismoelectric conversion in fluid-saturated porous medium, *66th SEG Annual International Meeting Expanded Abstracts, RP1.6,* 1699–1702.

Zhu, Z., and Toksöz, M.N., 1997, Experimental studies of electrokinetic conversion in fluid-saturated borehole models, *67th SEG Annual International Meeting Expanded Abstracts, Paper BH3.13*, 334–337.

Zhu, Z., and Toksöz, M.N., 1998, Seismoelectric measurements in a fractured borehole model, *68th SEG Annual International Meeting Expanded Abstracts, Paper BH2.7*, 314–317.

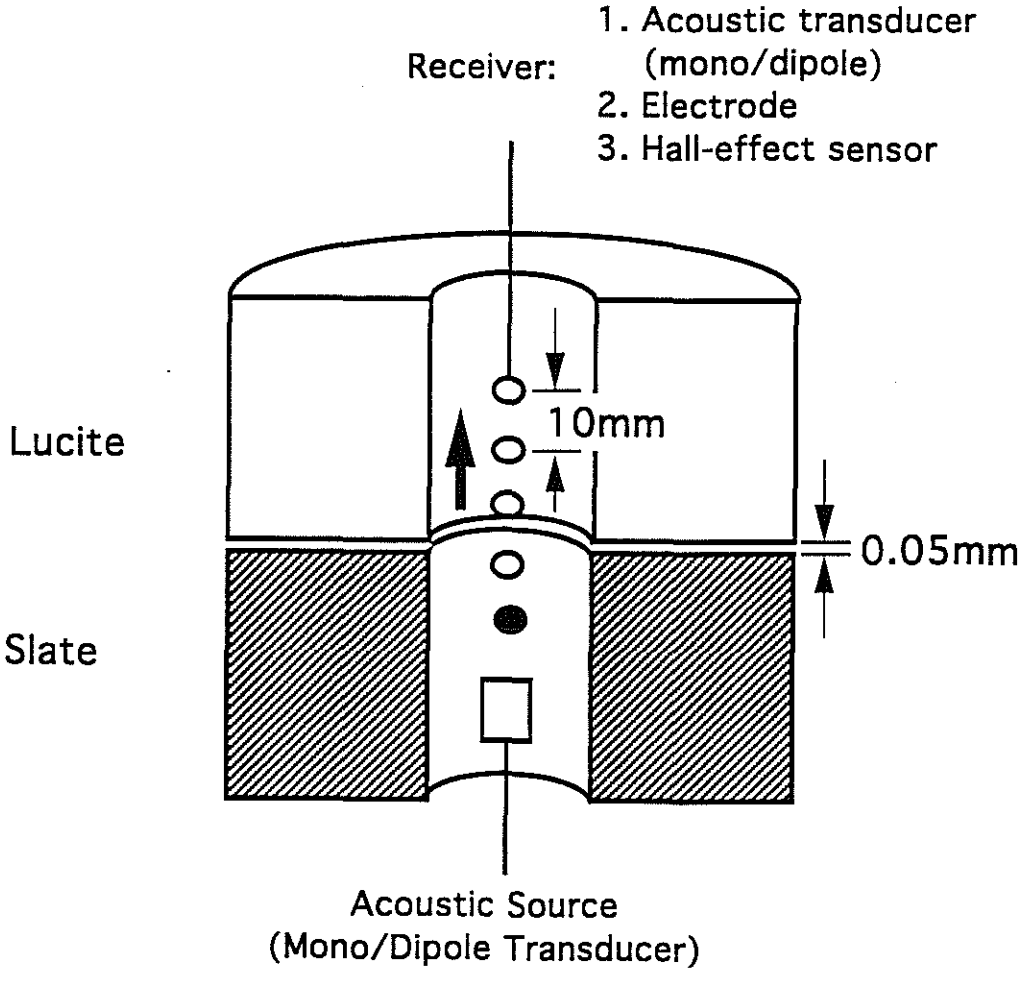

Figure 1: A water-saturated borehole model with a horizontal fracture between slate and Lucite. The diameter of the borehole is 1.0 cm. The aperture of the fracture is about 0.05 mm. The conductivity of the saturant (water) is 65 μS.

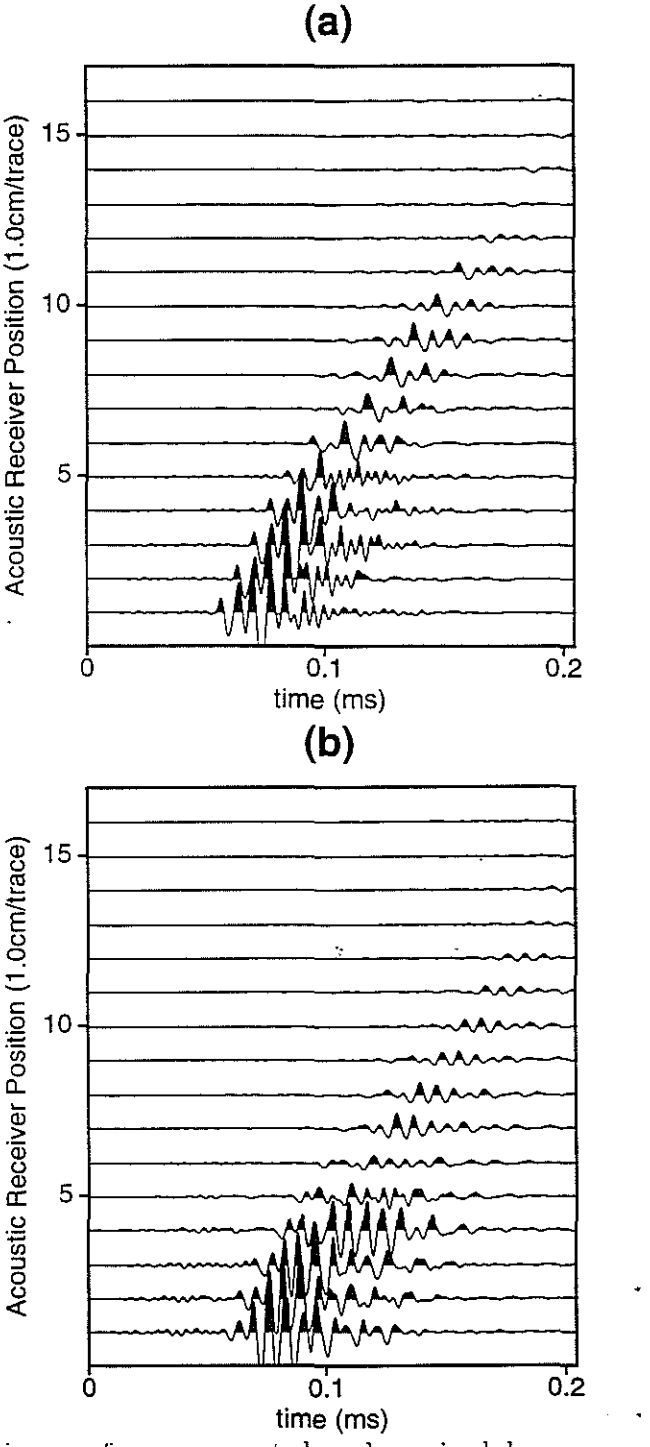

Figure 2: Acoustic waveforms generated and received by monopole (a) and dipole (b) transducers in a borehole with a horizontal fracture. The fracture, between slate and Lucite, is located between traces 5 and 6. The waveforms are recorded with 32 μs time delay and normalized for each plot.

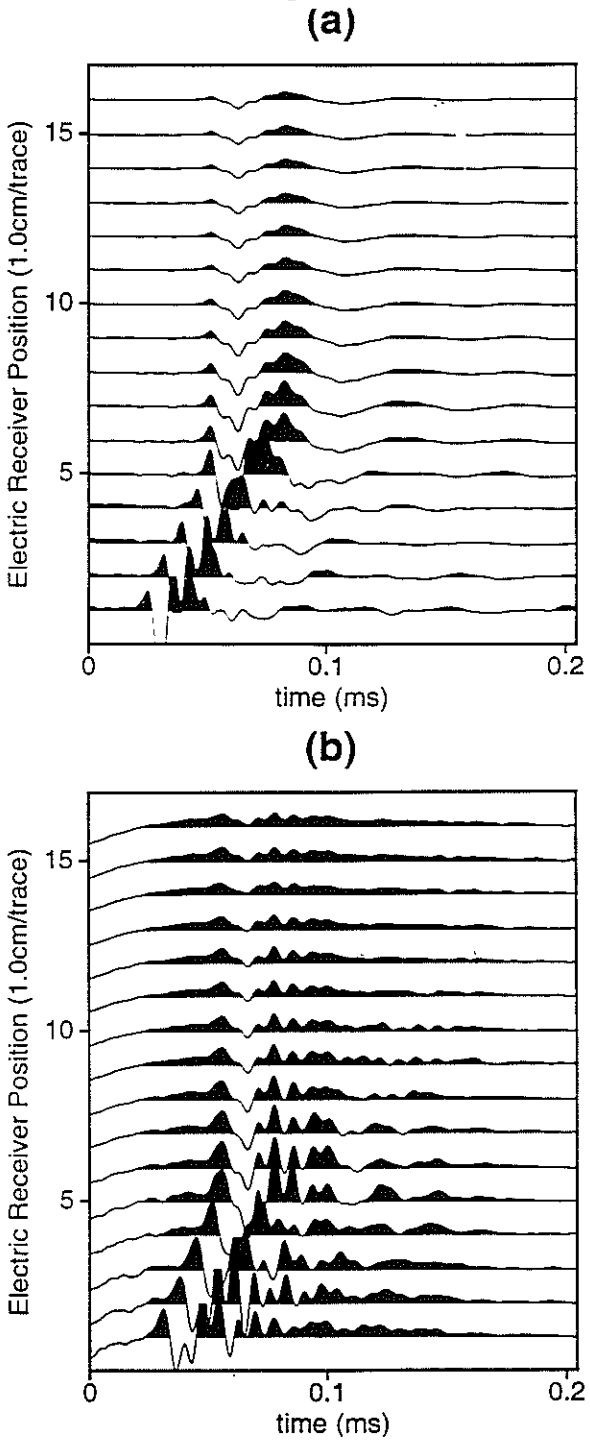

Figure 3: Seismoelectric signals generated by monopole (a) and dipole (b) sources in a borehole model with a horizontal fracture. The waveforms are normalized for each plot and recorded with 64 μs time delay (all of the following waveforms are taken with 64 μs time delay).

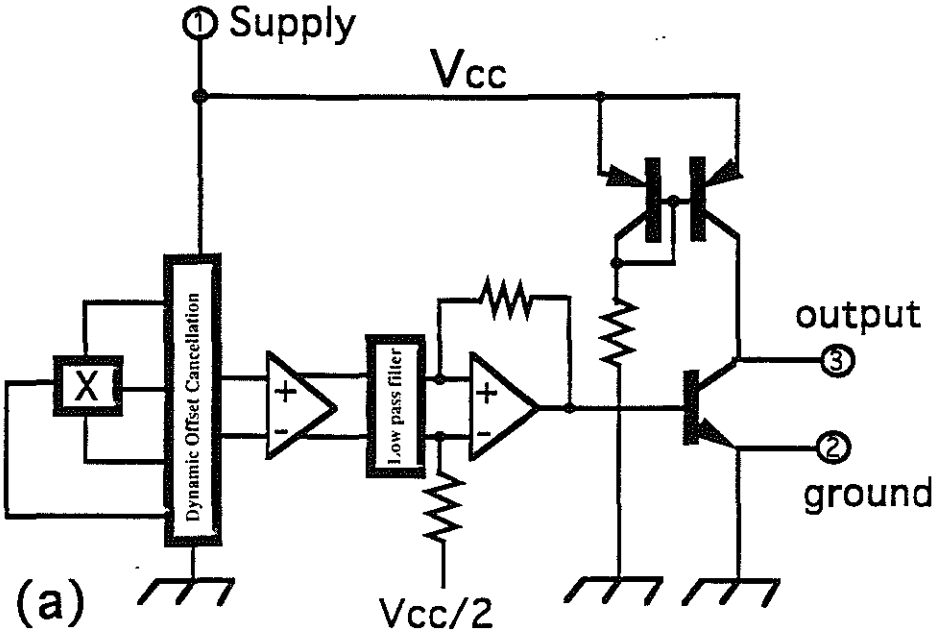

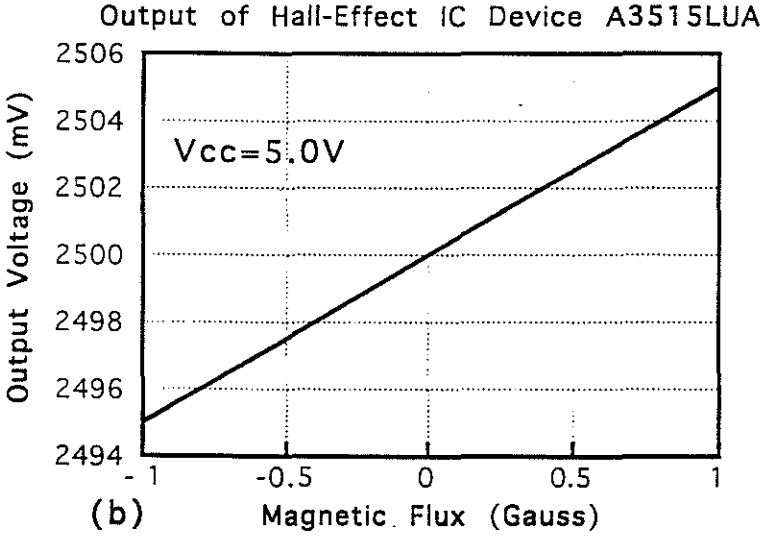

Figure 4: (a) Functional diagram of a linear Hall-effect device A3515 (Allegro MicroSystem, Inc.). The square with × indicates the Hall-effect sensor. (b) The linear relationship between the output of the Hall-effect device A3515LUA and the magnetic flux density (Allegro MicroSystem, Inc.).

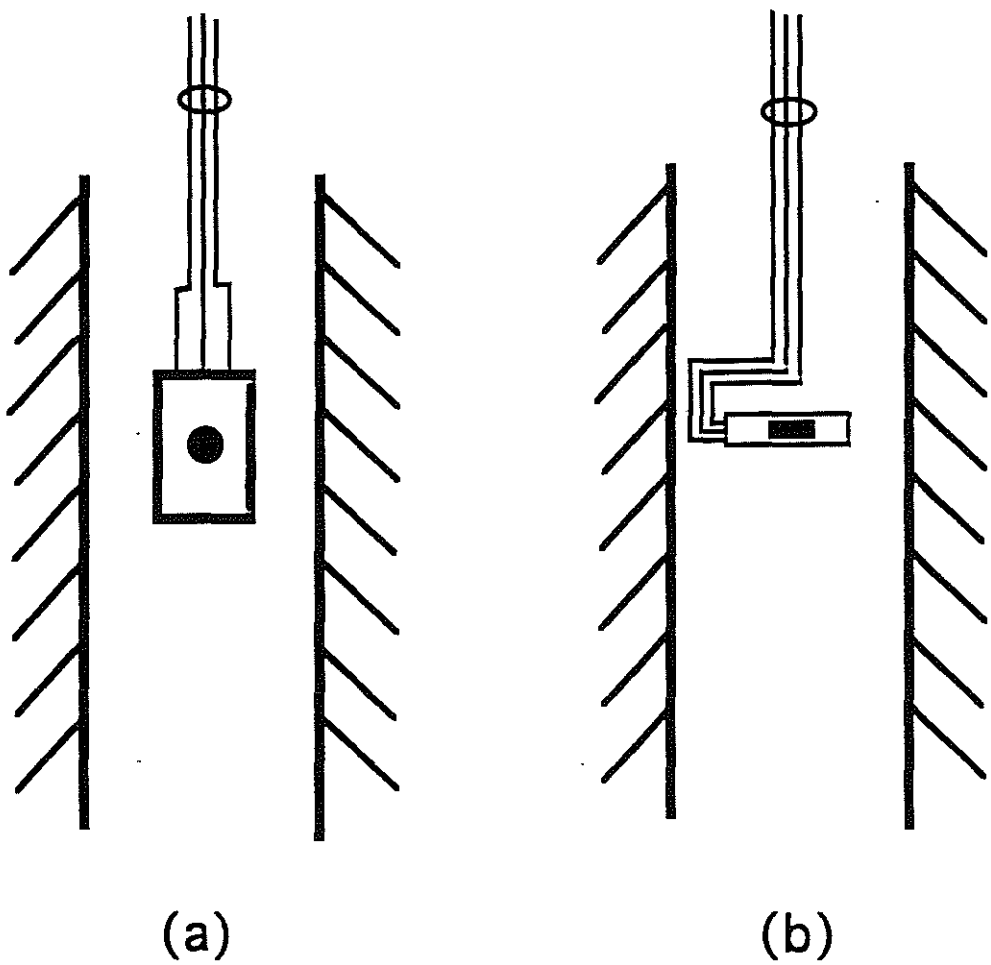

Figure 5: Diagram of the vertical (a) and horizontal (b) positions of the Hall-effect device in a borehole.

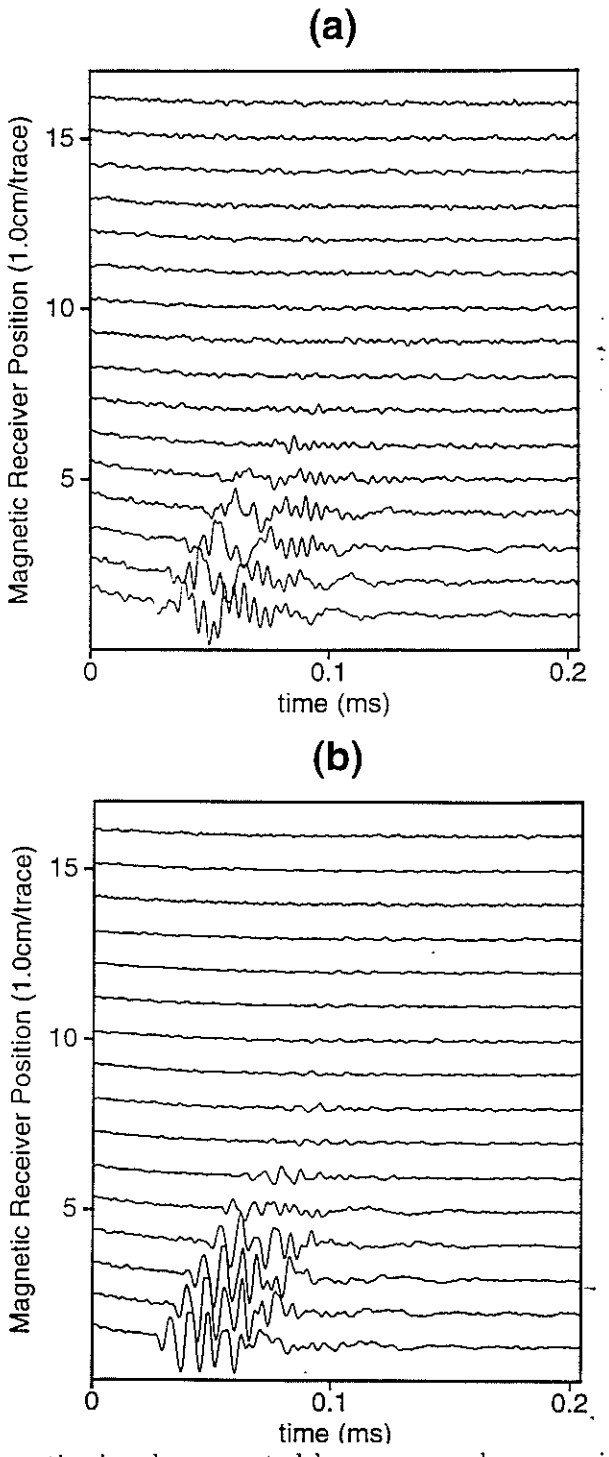

Figure 6: Seismomagnetic signals generated by a monopole source in the borehole with horizontal fracture and received by the Hall-effect device in vertical (a) and horizontal (b) positions. The maximum amplitude is about 10 μV. The center frequency is about 120 kHz.

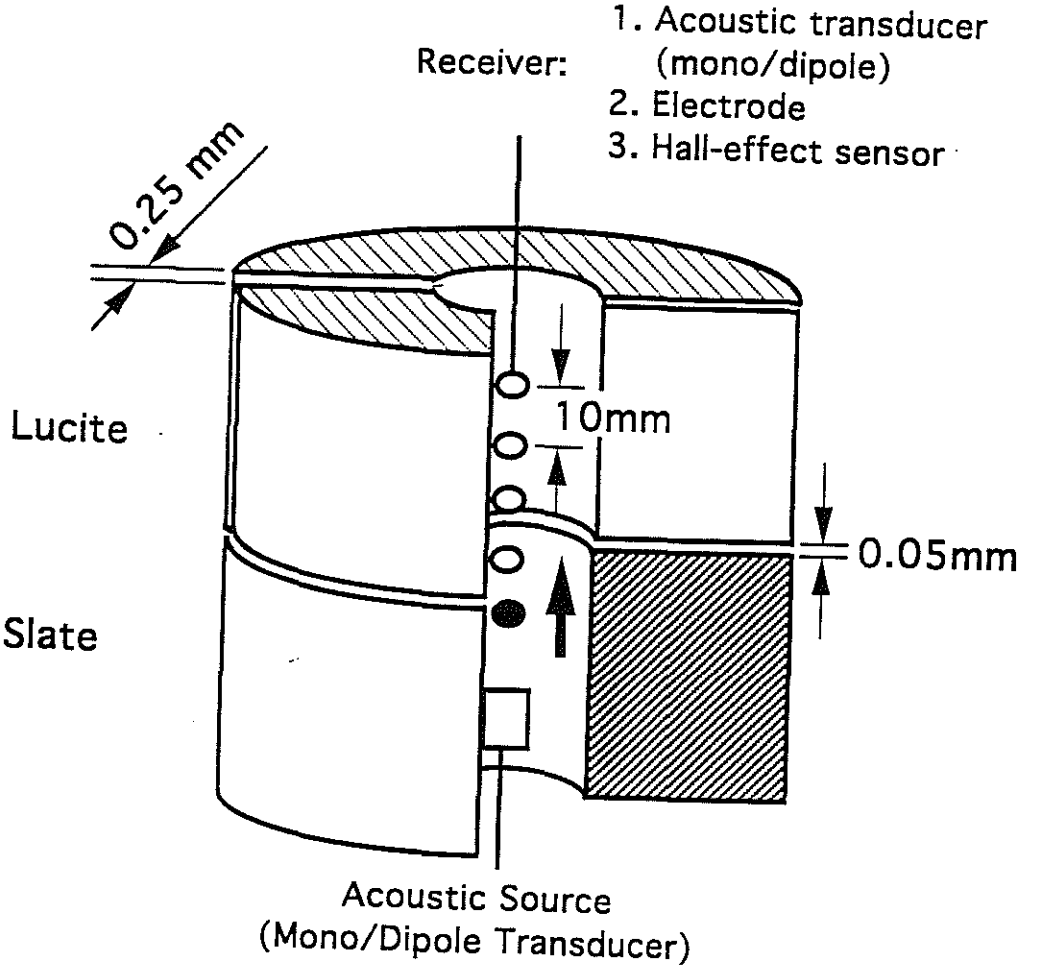

Figure 7: A water-saturated borehole model with a horizontal fracture between slate and Lucite and a vertical fracture in Lucite section. The diameter of the borehole is 1.0 cm. The apertures of the horizontal and vertical fractures are about 0.05 mm and 0.25 mm, respectively. The conductivity of the saturant (water) is 65 μS.

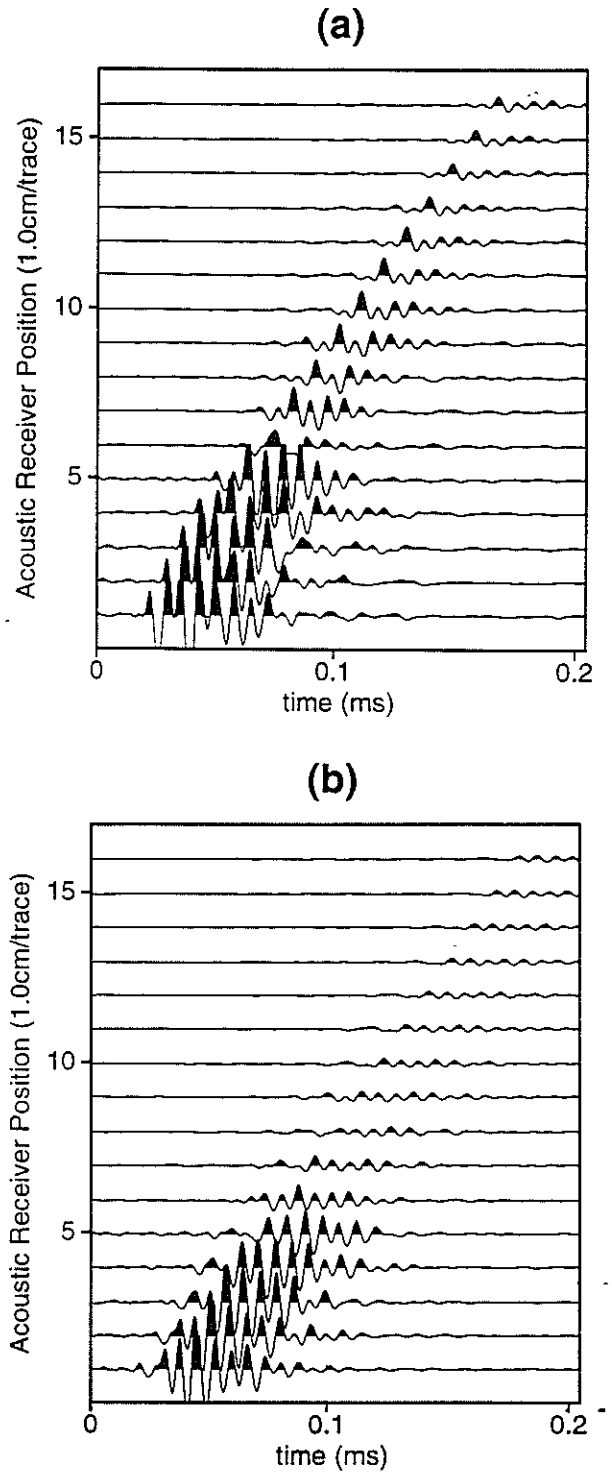

Figure 8: Acoustic waveforms generated and received by monopole (a) and dipole (b) transducers in the borehole model of Figure 7.

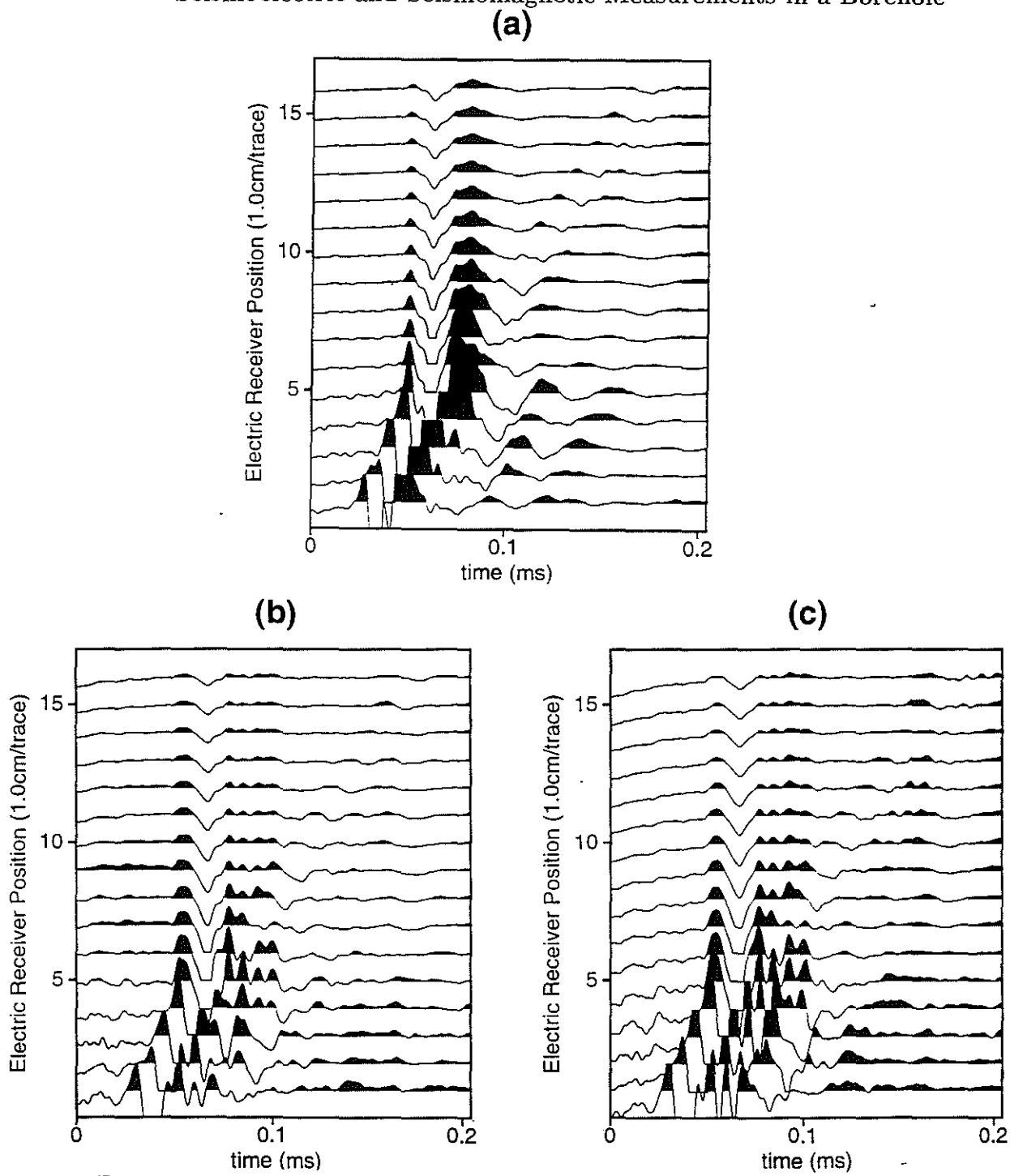

Figure 9: Seismoelectric signals generated by monopole (a) and dipole (b and c) sources in a borehole model with a vertical fracture shown in Figure 7. The signals shown in Figures 9b and 9c are recorded where the plane of the vertical fracture is parallel (Figure 9b) or perpendicular (Figure 9c) to the direction of the dipole source.

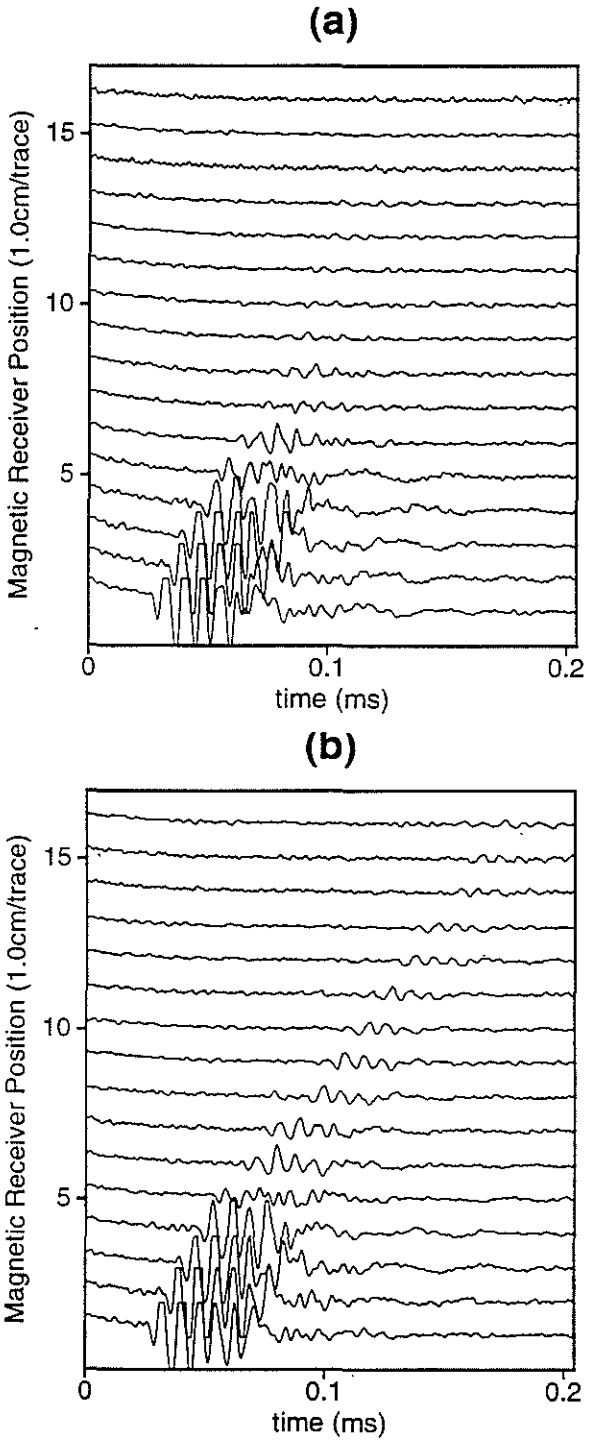

Figure 10: Seismomagnetic signals generated by a monopole source in the borehole with a vertical fracture and received by the Hall-effect device in vertical (a) and horizontal (b) positions. The magnetic field recorded in Lucite section (traces 60-16) propagates with the velocity of the Stoneley wave in Lucite.